

Electronic structure and photoinduced effect of LaMnO₃ film

K. Murakami, T. Yamauchi, and A. Nakamura

Department of Applied Physics, Nagoya University, Nagoya 464-8603, Japan

Y. Moritomo*

Department of Physics, University of Tsukuba, Tsukuba 305-8571, Japan

H. Tanaka and T. Kawai

Institute of Scientific and Industrial Research, Osaka University, Osaka 567-0047, Japan

(Received 1 May 2006; published 23 May 2006)

The electronic structure as well as the photoinduced effect were investigated in an antiferromagnetic LaMnO₃ film. We found characteristic spin-dependent absorption bands at ≈ 1.6 eV and ~ 3 eV, and ascribed them to the $d-d$ transitions into the adjacent Mn³⁺ sites with the parallel and antiparallel spins, respectively. We further observed that the photoexcitation of the down-spin d electrons significantly influences these $d-d$ bands, and ascribed the behavior to the photoinduced disorder of the Mn³⁺ spins.

DOI: [10.1103/PhysRevB.73.180403](https://doi.org/10.1103/PhysRevB.73.180403)

PACS number(s): 68.35.Rh, 75.40.-s

The photoinduced effects on the strongly correlated electron system¹⁻¹⁰ is one of the hottest topics in solid state physics both from the fundamental and technical points of view. Especially in the perovskite-type doped manganites, the strong coupling between the spin, charge and orbital degree of freedoms causes a variety of magnetic/electronic phases.¹¹ Reflecting the strong coupling, the photoexcitation of the d electrons significantly influences the other degrees of freedoms. For example, Ogasawara *et al.* reported a photoinduced melting of the charge/orbital ordering in La_{1/2}Sr_{3/2}MnO₄ (Ref. 1) and Nd_{1/2}Ca_{1/2}MnO₃ (Ref. 2). On the other hand, Matsuda *et al.*³ found a photoinduced disorder of the t_{2g} spins in ferromagnetic (Nd,Sm)_{0.6}Sr_{0.4}MnO₃. They ascribed the photoinduced effect to the strong on-site Hund's-rule coupling between the local t_{2g} spins and the photoexcited down-spin e_g electrons. Here, we have investigated the photoinduced effect of an antiferromagnetic LaMnO₃ with a layered-type spin structure.

The nondoped LaMnO₃ is known to show the $d_{3x^2-r^2}/d_{3y^2-r^2}$ orbital ordering¹² below T_{OO} (≈ 780 K), accompanying the cooperative Jahn-Teller distortion of the MnO₆ octahedron. This orbital alternation mediates the ferromagnetic exchange coupling within the ab plane, and causes the layer-type spin structure^{13,14} below T_N (≈ 140 K). The hole-doping process in LaMnO₃ induces the ferromagnetism, which is mediated by strong on-site exchange coupling J_H between the local t_{2g} spins and itinerant e_g carriers (double-exchange interaction¹⁵). This strong coupling *a priori* splits the e_g band into the parallel spin state and the antiparallel spin state. Actually, Moritomo *et al.*¹⁶ have observed the spin-dependent absorption band at J_H (≈ 3 eV) in several ferromagnetic manganite films, and ascribed the band to the $d-d$ transition between the exchange-split bands (J -gap transition). The corresponding absorption band is also expected in the insulating LaMnO₃. The interpretation of the electronic structure of LaMnO₃, however, is still controversial, even though there exists a long list of experimental¹⁷⁻²² and theoretical²²⁻²⁵ investigations. Quijada *et al.*¹⁸ investigated the optical conductivity spectrum of crystalline LaMnO₃

against temperature, and found a characteristic transfer of the spectral weight from the ultraviolet region (≥ 3 eV) to the visible region (~ 2 eV). They ascribed the former (latter) absorption to the $d-d$ transition into the Mn³⁺ site with the parallel (antiparallel) spin. Contrary to this argument, Tobe *et al.*¹⁷ reported that the anisotropic optical conductivity spectrum of LaMnO₃ crystal shows negligible change at T_N . Recently, Kovaleva *et al.*²¹ reported spin-dependent transition at ≈ 2 eV in untwinned LaMnO₃ crystal, and Kim *et al.*²² reported distinct suppression of the absorption band at ≈ 2 eV around T_N in the epitaxial LaMnO₃ film. In addition, several researchers^{27,26} observed spin-dependent excitation around 2 eV in doped and nondoped manganites by means of the resonant inelastic x-ray scattering experiments.

In this paper, we have investigated electronic structure as well as the photoinduced effect of LaMnO₃ film. We observed temperature-dependent absorption bands at ≈ 1.6 eV and ~ 3 eV. We further observed that the photoexcitation of the down-spin d electrons significantly suppresses (enhances) the lower-lying (higher-lying) $d-d$ band, and ascribed the behavior to the photoinduced disorder of the Mn³⁺ spins.

A LaMnO₃ film was fabricated using a laser molecular-beam epitaxy method on a SrTiO₃ (100) substrate. Details of the synthesis process were described elsewhere.²⁸ An x-ray diffraction measurement revealed that the obtained films were (001) oriented in the pseudo-tetragonal setting. That is, the ferromagnetic ab plane is parallel to the film surface. The Néel temperature T_N (≈ 60 K²⁹) was determined from the inflection point of the temperature dependence of the magnetization M , which was measured at 0.1 T after cooling down to 5 K in the zero field. The absorption coefficient $\alpha(\omega)$ was determined from transmission spectra using the standard formula neglecting the multi-reflection effect. The film thickness was 1790 Å. The transmission spectra were measured with a grating-type spectrometer. Reflectance correction is not performed, since the reflectivity ($R \sim 0.15$) is low and nearly constant in the spectral region investigated (0.6–3.1 eV).³⁰ Here, note that the spectral region is limited by absorption of the SrTiO₃ substrate.

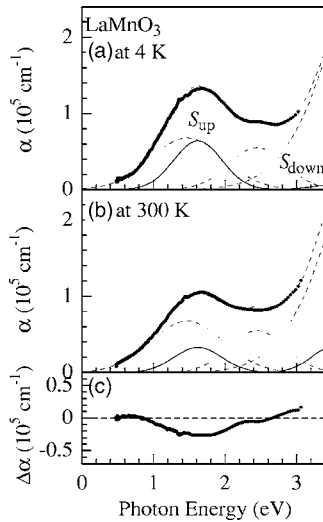


FIG. 1. Absorption spectra of LaMnO₃ film at (a) 4 K and at (b) 300 K. Thin solid curves represent the d - d transitions, while thin broken curves represent the charge-transfer (CT) transition. S_{up} (S_{down}) stands for the d - d transition into the adjacent Mn³⁺ site with the parallel (antiparallel) spin. The bottom figure (c) represents temperature differential spectrum ($\Delta\alpha = \alpha_{300 \text{ K}} - \alpha_{4 \text{ K}}$).

We used a nanosecond optical parametric oscillator system pumped by a yttrium-aluminum-garnet (YAG) laser (355 nm, 10 Hz) as an excitation source. The pulse width was 3–5 ns. We confirmed that the SrTiO₃ (100) substrate does not show any photoinduced signal, when the excitation photon energy was set below the absorption edge (≈ 3.1 eV) of the SrTiO₃ substrate. In the time-resolved spectroscopy, a xenon flush lamp was synchronized with the YAG laser. The transmitted light was detected with a gated charge-coupled device camera attached at the output stage of a grating monochromator. We put a polarizer in front of the monochromator to eliminate the intense scattering from the excitation light. The time resolution of the system was 12 ns. In order to obtain the overall temporal behavior of the photoinduced absorption change, we used continuous wave lasers, i.e., He-Ne laser (1.95 eV) and He-Cd laser (2.81 eV), as probe light sources. The intensities $I(t)$ of the transmitted light were detected with a P-intrinsic-N photodiode, and its temporal behavior was accumulated with a digital oscilloscope.

We first carefully investigated the temperature dependence of the absorption spectra of the LaMnO₃ film. Figure 1 shows a prototypical example of the absorption spectra at (a) 4 K ($\ll T_N$) and at (b) 300 K ($\gg T_N$). Consistent with the work done by Quijada *et al.*,¹⁸ we observed a characteristic transfer of the spectral weight from the ultraviolet region to the visible region. Figure 1(c) shows temperature differential spectrum of the LaMnO₃ film, which shows negative (positive) component at ≈ 1.6 eV and (~ 3.0 eV), even though the spectral region was limited below 3.1 eV. For convenience of explanation, we will call the lower-lying (higher-lying) component S_{up} (S_{down}). The peak position $\hbar\omega_0$ and the full width at half maximum Γ of the S_{up} component show negligible temperature-dependence. So, we expressed the two components by Gaussians, that is, $\propto \exp[-4 \ln 2 (\frac{\hbar\omega - \hbar\omega_0}{\Gamma})^2]$,

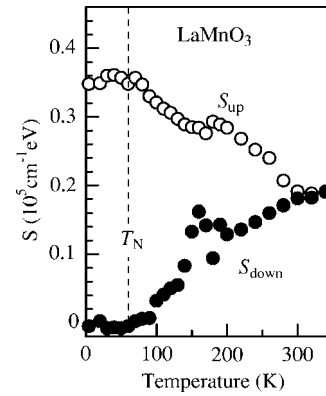


FIG. 2. Spectral weight of the S_{up} component and the S_{down} component of LaMnO₃ film. T_N stands for the Néel temperature.

where $\hbar\omega_0$ and Γ are the fixed values: $\hbar\omega_0 = 1.62$ eV (3.5 eV) and $\Gamma = 0.79$ eV (0.70 eV) for the S_{up} (S_{down}) component. Keeping these two components in mind, we decomposed the overall spectra into two temperature-dependent components (thin solid curves in Fig. 1) and three temperature-independent components (thin broken curves). The positions of the latter three components were chosen at $\hbar\omega_0 = 1.47, 2.44,$ and 4.5 eV so as to cover the spectra. The residual parameters, Γ and the spectral weight S , are adjusted so that the sum of the Gaussians reproduce the temperature-independent component except around ~ 1.6 eV and ~ 3 eV: $\Gamma = 1.20$ eV and $S = 1.22 \times 10^5 \text{ eV cm}^{-1}$ for the 1.47 eV component, $\Gamma = 0.93$ eV and $S = 0.72 \times 10^5 \text{ eV cm}^{-1}$ for the 2.44 eV component, and $\Gamma = 1.93$ eV and $S = 1.08 \times 10^6 \text{ eV cm}^{-1}$ for the 4.5 eV component. The temperature variation of the spectra can be reproduced only by the spectral weights of the S_{up} and S_{down} components.³¹ The three temperature-independent components located at 1.5, 2.4, and 4.5 eV are reasonably ascribed to the CT transitions into the $\text{Mn}_{g\uparrow}$, $\text{Mn}_{2g\downarrow}$ and $\text{Mn}_{g\downarrow}$ -levels, respectively.¹⁹

In Fig. 2, we plotted the spectral weights of the S_{up} component (open circles) and the S_{down} component (filled circles). As temperature increases beyond T_N , the spectral weight of the S_{up} component gradually transfers to the S_{down} component. These temperature dependencies are well explained if we ascribe the S_{up} (S_{down}) component to the d - d transition into the adjacent Mn³⁺ site with the parallel (antiparallel) spin. With increases of temperature above T_N , the probability of finding a parallel (antiparallel) spin pair within the ab plane decreases (increases), and eventually becomes the same ($=\frac{1}{2}$) in the paramagnetic phase. The rather gradual spectral weight transfer above T_N may be ascribed to the residual short-range ferromagnetic correlation. Here, we roughly estimated the oscillator strength f_{dd} of the d - d transition from the spectral weight of the S_{up} component.³² The magnitude of f_{dd} ($=0.04/e_g$ electron) is comparable with that ($f_{dd} = 0.05^{16}$) of the ferromagnetic $\text{Sm}_{0.5}\text{Sr}_{0.4}\text{MnO}_3$ film.

Figure 3(a) shows the differential absorption spectra $\Delta\alpha$ soon after the photoexcitation at 1.5 eV (gray spectrum) and at 2.3 eV (black spectrum). In both spectra, negative (positive) signal is observed at ≈ 1.6 eV (at ~ 3 eV), which is close to the S_{up} (S_{down}) component. So, we concluded that the photoexcitation modifies the spectral weights of the d - d tran-

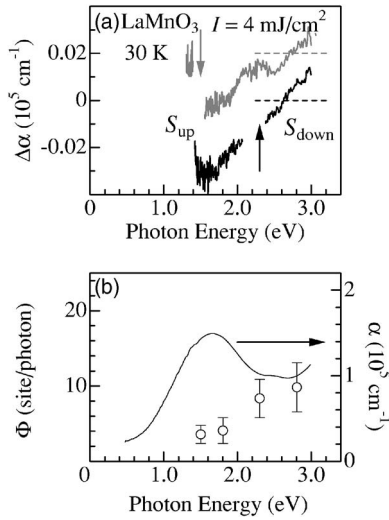


FIG. 3. (a) Differential absorption spectra $\Delta\alpha$ (at $\Delta t=0$ ns) of LaMnO_3 film at 30 K. Arrows represent the excitation photon energy E_{pump} . The excitation intensity I is 4 mJ/cm^2 . (b) Quantum efficiency Φ for the S_{up} component. A solid curve represents the absorption spectrum of LaMnO_3 film at 4 K.

sitions. The magnitude of the photoinduced spectral change is proportional to I up to $I=4 \text{ mJ/cm}^2$. We further estimated the quantum efficiency Φ for the S_{up} component and plotted them in Fig. 3(b), taking account of the reflectivity and transmittance at E_{pump} . Magnitude of Φ is nearly constant (~ 3 site/photon) below 2 eV, but jumps to ~ 8 site/photon when E_{pump} exceeds ~ 2 eV. This observation excludes the conventional heating effects as the origin for the photoinduced spectral change.

Matsuda *et al.*³ reported a similar excitation photon energy dependence in the photoinduced absorption at the J -gap transition (~ 3 eV) in a ferromagnetic $(\text{Nd,Sm})_{0.6}\text{Sr}_{0.4}\text{MnO}_3$ film. In this system, the profile of $\Delta\alpha$ is analogous to the spectral change between the ferromagnetic and paramagnetic phases. In addition, the photoinduced signal disappears in the spin-disordered paramagnetic phase. Based on these observations, they concluded that the observed photoinduced effect is originated in the photoinduced spin disorder, which is much enhanced by the excitation of the down-spin d electrons. We think that the presently observed photoinduced effect is also ascribed to photoinduced disorder of the Mn^{3+} spins, because the enhancement of Φ [Fig. 3(b)] appears to correlate with the CT excitation of the down-spin d electrons. In addition, the photoinduced spectral change [Fig. 3(a)] was analogous to the spectral change [Fig. 1(c)] between the spin-ordered and spin-disordered phases.

Finally, let us discuss temperature dependence of the photoinduced signal. Figure 4(a) shows prototypical examples of temporal behavior of $\frac{\Delta T}{T}$ at $E_{\text{probe}}=1.95$ eV, which is equivalent to $\frac{I(t)-I_0}{I_0}$, where I_0 represent the intensity of the transmitted light without photoexcitation. Based on the above interpretation, the magnitude of $\frac{\Delta T}{T}$ is equivalent to the degree of photoinduced spin disorder. The $\frac{\Delta T}{T}-t$ curves are well reproduced by the single exponential function: $\Delta T/T = A \cdot \exp(-t/\tau) + C$, where A and τ are the amplitude and the

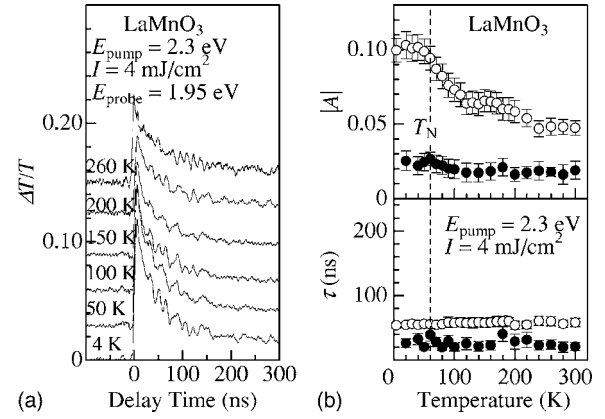


FIG. 4. (a) Relaxation curves of the relative transmittance change $\frac{\Delta T}{T}$ of LaMnO_3 film monitored at $E_{\text{probe}}=1.95$ eV. The excitation photon energy E_{pump} and the excitation intensity I were 2.3 eV and 4 mJ/cm^2 , respectively. (b) Temperature dependence of the amplitude A and the lifetime τ of LaMnO_3 film. Open (filled) circles represent the S_{up} (S_{down}) component monitored at $E_{\text{probe}}=1.95$ eV (2.81 eV). T_N stands for the Néel temperature.

lifetime, respectively. The constant term (C) is probably due to the heating effect, lasting for much longer time than the time range concerned here. Open circles in Fig. 4(b) represent A and τ for the S_{up} component. Magnitude of A is nearly constant below T_N , but gradually decreases as temperature increases beyond T_N . On the other hand, τ is almost temperature independent even near T_N . This is in sharp contrast with the $\text{La}_{0.7}\text{Ca}_{0.3}\text{MnO}_3$ film,⁴ in which τ critically slows down on approaching the Curie temperature T_C . Similar behaviors of A and τ are observed for the S_{down} component (indicated by filled circles), though the data points are rather scattered. These observations suggest that the local spin correlation does not change much even around T_N . Actually, Hirota *et al.*³³ observed ferromagnetic spin-wave-like dispersion for $E \geq 10$ meV even near T_N , indicating residual short-range ferromagnetic spin correlation due to two-dimensional exchange coupling. Here, note that the optical probe mainly detects the nearest-neighboring spin correlation. Then, it is plausible that the optical probe does not feel the long-range antiferromagnetic-paramagnetic phase transition of LaMnO_3 .

In summary, we have investigated the electronic structure as well as the photoinduced effect in an antiferromagnetic LaMnO_3 film. We decomposed the absorption spectra into three spin-independent CT components and two spin-dependent d - d components, and concluded that the charge gap has the CT character. We further observed that the photoexcitation significantly influences the spin-dependent d - d components due to the photoinduced disorder of the Mn^{3+} spins.

Temperature dependence of the photoinduced signal of LaMnO_3 is qualitatively different from that of the ferromagnetic $\text{La}_{0.7}\text{Ca}_{0.3}\text{MnO}_3$.

This work was supported by a Grant-in-Aid for Scientific Research from the Ministry of Education, Culture, Sports, Science and Technology, Japan, and from the Ookura Foundation.

- *Electronic address: moritomo@sakura.cc.tsukuba.ac.jp
- ¹T. Ogasawara, T. Kimura, T. Ishikawa, M. Kuwata-Gonokami, and Y. Tokura, *Phys. Rev. B* **63**, 113105 (2001).
 - ²T. Ogasawara, K. Tobe, T. Kimura, H. Okamoto, and Y. Tokura, *J. Phys. Soc. Jpn.* **71**, 2380 (2002).
 - ³K. Matsuda, A. Machida, Y. Moritomo, and A. Nakamura, *Phys. Rev. B* **58**, R4203 (1998).
 - ⁴X. J. Liu, Y. Moritomo, A. Machida, A. Nakamura, H. Tanaka, and T. Kawai, *Phys. Rev. B* **63**, 115105 (2001); X. J. Liu, Y. Moritomo, A. Nakamura, H. Tanaka, and T. Kawai, *Phys. Rev. B* **64**, 100401 (2001).
 - ⁵K. Miyano, T. Tanaka, Y. Tomioka, and Y. Tokura, *Phys. Rev. Lett.* **78**, 4257 (1997).
 - ⁶T. Kise, T. Ogasawara, M. Ashida, Y. Tomioka, Y. Tokura, and M. Kuwata-Gonokami, *Phys. Rev. Lett.* **85**, 1986 (2000).
 - ⁷X. J. Liu, Y. Moritomo, A. Machida, and A. Nakamura, *Jpn. J. Appl. Phys., Part 2* **39**, L670 (2000).
 - ⁸M. Sasaki, G. R. Wu, W. X. Gao, H. Negishi, M. Inoue, and G. C. Xiong, *Phys. Rev. B* **59**, 12425 (1999).
 - ⁹S. A. McGill, R. I. Miller, O. N. Torrens, A. Mamchik, I.-Wei Chen, and J. M. Kikkawa, *Phys. Rev. B* **71**, 075117 (2005).
 - ¹⁰M. Fiebig, K. Miyano, Y. Tomioka, and Y. Tokura, *Science* **280**, 1925 (1998).
 - ¹¹Y. Tokura and N. Nagaosa, *Science* **288**, 462 (2000).
 - ¹²Y. Murakami, J. P. Hill, D. Gibbs, M. Blume, I. Koyama, M. Tanaka, H. Kawata, T. Arima, Y. Tokura, K. Hirota, and Y. Endoh, *Phys. Rev. Lett.* **81**, 582 (1998).
 - ¹³E. O. Wollan and W. C. Koehler, *Phys. Rev.* **100**, 545 (1955).
 - ¹⁴G. Matsumoto, *J. Phys. Soc. Jpn.* **29**, 606 (1970).
 - ¹⁵P. W. Anderson and H. Hasegawa, *Phys. Rev.* **100**, 675 (1955).
 - ¹⁶Y. Moritomo, A. Machida, K. Matsuda, M. Ichida, and A. Nakamura, *Phys. Rev. B* **56**, 5088 (1997).
 - ¹⁷K. Tobe, T. Kimura, Y. Okimoto, and Y. Tokura, *Phys. Rev. B* **64**, 184421 (2001).
 - ¹⁸M. A. Quijada, J. R. Simpson, L. Vasiliu-Doloc, J. W. Lynn, H. D. Drew, Y. M. Mukovskii, and S. G. Karabashev, *Phys. Rev. B* **64**, 224426 (2001).
 - ¹⁹T. Arima, Y. Tokura, and J. B. Torrance, *Phys. Rev. B* **48**, 17006 (1993).
 - ²⁰J. H. Jung, K. H. Kim, T. W. Noh, E. J. Choi, and J. Yu, *Phys. Rev. B* **57**, R11043 (1998).
 - ²¹N. N. Kovaleva, A. V. Boris, C. Bernhard, A. Kulakov, A. Pimenov, A. M. Balbashov, G. Khaliullin, and B. Keimer, *Phys. Rev. Lett.* **93**, 147204 (2004).
 - ²²M. W. Kim, P. Murugavel, S. Parashar, J. S. Lee, and T. W. Noh, *New J. Phys.* **6**, 156 (2004).
 - ²³I. Solovyev, N. Hamada, and K. Terakura, *Phys. Rev. B* **53**, 7158 (1995).
 - ²⁴K. H. Ahn and A. J. Millis, *Phys. Rev. B* **61**, 13545 (2000).
 - ²⁵V. Perebeinos and P. B. Allen, *Phys. Rev. Lett.* **85**, 5178 (2000).
 - ²⁶S. Grenier, J. P. Hill, V. Kiryukhin, W. Ku, Y.-J. Kim, K. J. Thomas, S.-W. Cheong, Y. Tokura, Y. Tomioka, D. Casa, and T. Gog, *Phys. Rev. Lett.* **94**, 047203 (2005).
 - ²⁷T. Inami, T. Fukuda, J. Mizuki, S. Ishihara, H. Kondo, H. Nakao, T. Matsumura, K. Hirota, Y. Murakami, S. Maekawa, and Y. Endoh, *Phys. Rev. B* **67**, 045108 (2003).
 - ²⁸M. Kanai, H. Tanaka, and T. Kawai, *Phys. Rev. B* **70**, 125109 (2004).
 - ²⁹ T_N of our LaMnO_3 film is lower than that (≈ 140 K) of the LaMnO_3 bulk. This may be due to the slight oxygen deficiency, because the film was synthesized in a moderate oxidizing atmosphere in order to avoid the cation deficiencies.
 - ³⁰The temperature change of the absolute reflectivity was less than 1.5% in the spectral range of 0.7–3.0 eV. The resultant error in the absorption coefficient α is $\pm 0.01 \times 10^5 \text{ cm}^{-1}$, which is much smaller than α and $\Delta\alpha$ (see Fig. 1).
 - ³¹The absolute magnitude of S_{down} has ambiguity due to the limitation of the spectral range.
 - ³²The refractive index n of LaMnO_3 is ~ 2 in the visible region.¹⁹
 - ³³K. Hirota, N. Kaneko, A. Nishikawa, and Y. Endo, *J. Phys. Soc. Jpn.* **65**, 3736 (1996).